Introduction of a $\pi-\pi$ Interaction at the Active Site of a Cupredoxin: Characterization of the Met16Phe Pseudoazurin Mutant†

Sachiko Yanagisawa,‡ Katsuko Sato,‡ Makiko Kikuchi,§ Takamitsu Kohzuma,*,§ and Christopher Dennison*,‡

School of Natural Sciences, Bedson Building, University of Newcastle upon Tyne, Newcastle upon Tyne, NE1 7RU, United Kingdom, and Department of Materials and Biological Science, Faculty of Science, Ibaraki University, Mito, Ibaraki 310-8512, Japan

Received February 4, 2003; Revised Manuscript Received April 11, 2003

ABSTRACT: The Met16Phe mutant of the type 1 copper protein pseudoazurin (PACu), in which a phenyl ring is introduced close to the imidazole moiety of the His81 ligand, has been characterized. NMR studies indicate that the introduced phenyl ring is parallel to the imidazole group of His81. The mutation has a subtle effect on the position of the two S(Cys)→Cu(II) ligand-to-metal charge transfer bands in the visible spectrum of PACu(II) and a more significant influence on their intensities resulting in a A_{459}/A_{598} ratio of 0.31 for Met16Phe as compared to a A_{453}/A_{594} ratio of 0.43 for wild-type PACu(II) at pH 8. The electron paramagnetic resonance spectrum of the Met16Phe variant is more axial than that of the wild-type protein, and the resonance Raman spectrum of the mutant exhibits subtle differences. A $C^{\gamma}H$ proton of Met86 exhibits a much smaller hyperfine shift in the paramagnetic ^1H NMR spectrum of Met16Phe PACu(II) as compared to its position in the wild-type protein, which indicates a weaker axial Cu−S(Met86) interaction in the mutant. The Met16Phe mutation results in an ∼60 mV increase in the reduction potential of PACu. The pK_a value of the ligand His81 decreases from 4.9 in wild-type PACu(I) to 4.5 in Met16Phe PACu(I) indicating that the $\pi-\pi$ contact with Phe16 stabilizes the Cu−N(His81) interaction. The Met16Phe variant of PACu has a self-exchange rate constant at pH* 7.6 (25 °C) of 9.8×10^3 M^{-1} s^{-1} as compared to the considerably smaller value of 3.7×10^3 M^{-1} s^{-1} for the wild-type protein under identical conditions. The enhanced electron transfer reactivity of Met16Phe PACu is a consequence of a lower reorganization energy due to additional active site rigidity caused by the $\pi-\pi$ interaction between His81 and the introduced phenyl ring.

Type 1 copper sites are found in a wide range of proteins and are always involved in ET[1] reactions. Single domain proteins that bind a solitary type 1 copper ion as their only cofactor are known as cupredoxins. PACu is a cupredoxin, which is found in denitrifying bacteria where it acts as the electron donor to a NiR (*1*−*3*). The structures of PACu from various sources have been determined (*4*−*10*). In all cases, the protein contains eight β-strands, which form two β-sheets giving an overall β-sandwich topology. Additionally, PACu possesses two α-helices, which are located at its C terminus. The single copper ion is buried approximately 5 Å from the protein surface and has a distorted tetrahedral geometry, with the metal strongly coordinated by the N^{δ} atoms of His40 and His81 and by the thiolate sulfur of Cys78 (see Figure 1). The copper ion is displaced from the plane of these three equatorial ligands by ∼0.4 Å in the direction of the thioether sulfur of the weak axial Met86 ligand. The C-terminal His81 ligand of PACu protrudes through a region on the protein's

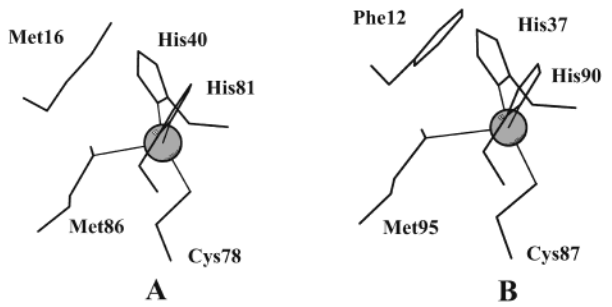

FIGURE 1: Active site structure of (A) PACu(II) from *A. cycloclastes* (*8*) (PDB accession code 1BQK) and (B) oxidized plastocyanin from the fern *D. crassirhizoma* (*11*, *12*) (PDB accession code 1KDJ) drawn with MOLSCRIPT (*13*). In both structures, the four coordinating residues are shown along with the side chain of the amino acid that interacts with the imidazole ring of the C-terminal His ligand. The copper ion is shown as a gray sphere in both structures.

† C.D. thanks Newcastle University and the Royal Society for funding, Universities UK for ORS awards to both S.Y. and K.S., and EPSRC for a grant to purchase the NMR spectrometer. T.K. and C.D. thank the Ministry of Education, Culture, Sports, Science and Technology of Japan for a grant (13640553).

* To whom correspondence should be addressed. (C.D.) Tel: +44 191 222 7127. Fax: +44 191 222 6929. E-mail: christopher.dennison@ncl.ac.uk. (T.K.) Tel: +81 029 228 8372. Fax: +81 029 228 8403. E-mail: kohzuma@biomol.sci.ibaraki.ac.jp.

‡ University of Newcastle upon Tyne.

§ Ibaraki University.

[1] Abbreviations: ET, electron transfer; PACu, pseudoazurin; PACu(I), reduced pseudoazurin; PACu(II), oxidized pseudoazurin; NiR, nitrite reductase; ESE, electron self-exchange; LMCT, ligand-to-metal charge transfer; EPR, electron paramagnetic resonance; Met16Phe, the Met16 → Phe mutant of pseudoazurin; wt, wild type; UV/vis, ultraviolet/visible; BCA, bicinchonic acid; Hepes, 4-(2-hydroxyethyl)-piperazine-1-ethanesulfonic acid; RR, resonance Raman; NMR, nuclear magnetic resonance; pH*, pH meter reading uncorrected for the deuterium isotope effect; NHE, normal hydrogen electrode; Mes, 2-morpholinoethanesulfonic acid; HSE, Hahn spin−echo; CPMG, Carr−Purcell−Meiboom−Gill; TOCSY, total correlation spectroscopy; NOESY, nuclear Overhauser enhancement spectroscopy.

10.1021/bi030030p CCC: $25.00
Published on Web 05/10/2003

surface made up of nonpolar amino acid residues, an area crucial for the association of PACu, and other cupredoxins, with physiological redox partners (*14*−*17*). The hydrophobic patch has also been shown to be the region whereby two cupredoxins associate to form the encounter complex for ESE (*18*−*20*).

Type 1 copper sites, such as that found in PACu, have unique spectroscopic features including an intense S(Cys)→Cu(II) LMCT transition at ∼600 nm in their visible spectra and unusually small A_z values in their EPR spectra (*21*, *22*). Site-directed mutagenesis studies have demonstrated that the only active site residue required for a copper center with type 1 spectroscopic properties is the Cys ligand (*21*, *23*). The replacement of the other coordinating amino acids results in a type 1 copper site with slightly altered spectroscopic features (*21*, *24*−*33*). In almost all cases, mutation of one of the ligating residues results in dramatically decreased ET reactivity.

Because of the elaborate design of cupredoxins, it is not only the coordinating residues that are of key importance to the structure and function of the copper center. The second coordination sphere of the metal ion is essential for producing an efficient ET protein by helping to maintain a rigid active site environment [the concept of an entatic (*34*) or rack-induced (*35*) state]. One such vital residue is the Asn, which is found adjacent to the N-terminal His ligand in most cupredoxins and makes a number of important hydrogen-bonding contacts in the vicinity of the copper site. These interactions enhance the stiffness of the protein in this region, and mutagenesis studies have highlighted the importance of this residue (*36*−*38*). Another key residue present in the second coordination sphere of certain cupredoxins is the Pro, which is found immediately before the C-terminal His ligand. In PACu, it has been shown that the Pro80Ala and Pro80Ile mutations both affect the reduction potential of the protein (*39*, *40*). In the Pro80Ala mutant, this influence has been attributed to a change in the solvation energy of the copper center, whereas the modification in the reduction potential observed in the Pro80Ile variant is mainly due to geometric effects (*40*). Mutation of the corresponding residue in amicyanin (Pro94) also has a significant influence on the reduction potential of this cupredoxin (*41*).

The interaction of ligating amino acids at a type 1 copper site with aromatic residues in the second coordination sphere of the metal ion is also important (*11*, *12*, *42*−*45*). One recently identified example is a novel cation−π interaction, a noncovalent contact important in numerous biological systems (*46*), between the ligand His39 and Phe13 in the cupredoxin cucumber basic protein (*45*). Another noncovalent interaction involving the ligating imidazoles and aromatic side chains, which has recently been identified in a cupredoxin, is a $\pi-\pi$ interaction (*11*, *12*). Attractive $\pi-\pi$ interactions have been appreciated for many years and are key factors in the structure of DNA (*47*), DNA intercalation (*48*), the three-dimensional structures of proteins (*49*), and numerous other biological and chemical systems (for example, see refs *50*−*55*). Of particular interest for the present investigations are the studies on Cu(II)(His)(amino acid−Phe, Tyr, or Trp) complexes, which show the existence of intramolecular stacking between the imidazole ring of the coordinated His and the particular aromatic side chain (*51*−*53*). In the plastocyanin (also a cupredoxin) from the fern *Dryopteris crassirhizoma*, a $\pi-\pi$ interaction between the C-terminal His90 ligand and the phenyl ring of Phe12 (see Figure 1) results in this protein having a number of unusual features (*11*, *12*, *56*). One such attribute is the absence of protonation and dissociation of the His ligand in the reduced protein in the accessible pH range, which occurs in all other plastocyanins (*56*, *57*) as well as in a number of other reduced cupredoxins including PACu (*6*, *58*−*62*). Protonation of the C-terminal His ligand has a dramatic effect on the reduction potential and ET capabilities of cupredoxins (*56*, *58*, *63*−*66*), and it has been purported that it may have physiological relevance (*57*, *62*, *66*).

In the structure of PACu, the solvent-exposed His81 interacts weakly with the side chain of Met16, which is within van der Waals contact distance (see Figure 1). In this study, we have introduced a $\pi-\pi$ interaction between the His81 ligand and the phenyl group of a Phe in PACu by constructing the Met16Phe variant. The intriguing influence that this noncovalent interaction has on the properties of the copper site of PACu is reported.

EXPERIMENTAL PROCEDURES

Growing Achromobacter cycloclastes and the Isolation of Native PACu. *A. cycloclastes* was grown, and native PACu was isolated and purified as described previously (*67*).

Cloning of the PACu Gene. *A. cycloclastes* IAM 1013 was grown at 30 °C in LB medium, and genomic DNA was isolated (using the G NOME kit from BIOgene). The genomic DNA was used as a template in polymerase chain reactions (PCR) in which the PACu gene was amplified using the following two primers: ccatggtgaatgcaatcaagag (forward primer) and ccatggctagaagtcgcttagt (reverse primer). The primer sequences were based on the DNA sequence of *A. cycloclastes* IAM 1013 PACu (*68*) and were designed in such a way to include the signal sequence for the protein. The amplified fragment was subcloned into pBluescript, digested with *NcoI*, and ligated into pTrc99A (Amersham). Both strands of the PACu insert in this plasmid (pTrcsPACu) were sequenced.

Introduction of the Met16Phe Mutation. Mutagenesis was carried out on the pTrcsPACu plasmid using the QuickChange (Stratagene) site-directed mutagenesis kit. The following primers were utilized to bring about the Met16Phe mutation: ggcaaggacggcgcgttcgttttcgagccggcg (forward primer) and cgccggctcgaaaacgaacgcgccgtccttgcc (reverse primer) with the underline codons corresponding to the introduced amino acid. The plasmid containing the mutation (pTrcM16F) was verified by sequencing.

Cell Growth, Protein Isolation, and Purification of Wild-Type and Met16Phe PACus. For both the wt PACu and the Met16Phe variant, the bacterial growth procedure and the method used for protein isolation and purification are identical and can be found in the Supporting Information.

UV/Vis Spectrophotometry. For UV/vis experiments, the proteins were fully oxidized using a sufficient volume of a 20 mM solution of $K_3[Fe(CN)_6]$. The proteins were exchanged into 10 mM potassium phosphate. UV/vis spectra were acquired at 25 °C on a Perkin-Elmer λ35 spectrophotometer at various pH values.

Determination of Molar Extinction Coefficients. To determine the molar extinction coefficients (ϵ values in M^{-1}

cm^{-1}) of the Met16Phe mutant, a protein solution of a certain concentration was prepared in 20 mM phosphate, pH 6.0. Three separate UV/vis spectra were obtained and averaged. Three independent protein concentrations were carried out using the BCA protein assay kit (Pierce). In this analysis, pure wt PACu was used to obtain the calibration plot.

EPR Spectroscopy. X-band EPR spectra were obtained on a frozen solution of both wt and Met16Phe PACu(II) at 77 K on either a JEOL RE3X or Bruker EMX spectrometer. The protein was exchanged into 25 mM Hepes, pH 7.6 (40% glycerol) and either 50 mM phosphate or 50 mM acetate for measurements in the ranges pH 5−10 and pH 3−5, respectively. Spectra were simulated using the program SIMFONIA (Bruker).

RR Spectroscopy. RR spectra were measured with samples in 20 mM phosphate at pH 7.0 and at room temperature with a spinning cell (1800 rpm; diameter = 5 mm). Raman shifts were calibrated to an accuracy of 1 cm^{-1} using CCl_4. RR scattering was excited at 647.1 nm using a Kr^+ ion laser (Spectra-Physics model 2016) and a liquid nitrogen-cooled CCD detector (Princeton Instruments, model LN/CCD-1100 × 300PB) attached to a single monochromator (Ritsu Oyo Kagaku model MC-100 DG). The laser power at the sampling point was adjusted to 20 mW.

Protein Samples for Paramagnetic ^1H NMR Studies. For the paramagnetic NMR experiments, PACu(II) samples were exchanged into 10 mM potassium phosphate in 99.9% D_2O at pH* 7.6 using centrifugal ultrafiltration units (Centricon 10, Amicon) and typically contained ∼3 mM protein.

PACu(I) Samples for ^1H NMR Investigations. PACu was fully reduced by the addition of 1 equiv of sodium ascorbate, and the protein was exchanged into 10 mM potassium phosphate (99.9% D_2O). The sample was transferred to an NMR tube and flushed with nitrogen. A small amount of sodium ascorbate was added to the sample to maintain the protein in the reduced form.

NMR Sample Preparation for ESE Rate Constant Measurements. For ESE rate constant measurements, Met16Phe PACu was exchanged into 37 mM phosphate at pH* 7.6. PACu(I) was produced as described above, with the excess reductant exchanged out by ultrafiltration. The reduced sample was placed in an NMR tube, flushed with nitrogen, and sealed. Fully oxidized protein was obtained as described above, and the excess oxidant was removed by ultrafiltration. Small amounts of the oxidized protein were added to the reduced sample. The concentration of PACu(II) was determined by transferring the mixed sample to a 2 mm UV/vis cuvette and measuring the absorbance at 598 nm ($\epsilon = 4700$ M^{-1} cm^{-1}). Readings were taken before and after the acquisition of NMR spectra, with an average of the two values used for all subsequent calculations (the values usually differed by <0.2% of the total protein concentration).

Adjustment of the pH of Protein Samples. The pH values of protein solutions were measured using a narrow pH probe (Russell KCMAW11) with an Orion 420A pH meter. The pH of the sample was adjusted using NaOD or DCl in deuterated solutions and NaOH and HCl in H_2O solutions. The pH values quoted in deuterated solutions are uncorrected for the deuterium isotope effect and are indicated by pH*.

NMR Spectroscopy. ^1H NMR spectra were acquired on a JEOL Lambda 500 spectrometer largely as described previously (*67*), and the details are given in the Supporting Information.

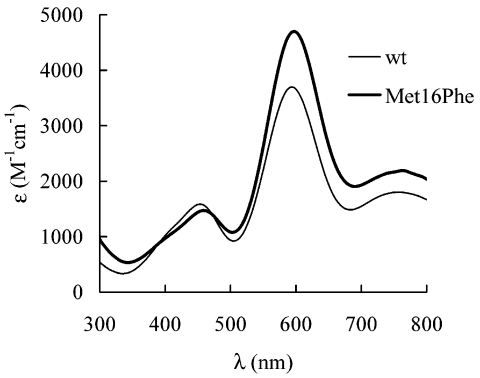

FIGURE 2: Part of the UV/vis spectra (25 °C) of the oxidized proteins at pH 8.0 in 10 mM phosphate.

Electrochemical Measurements. The direct measurement of the reduction potential of the Met16Phe variant was carried out using an electrochemical set up described previously (*11*) with a gold working electrode modified with 4,4-dithiodipyridine. The reduction potential at various pH values was measured at room temperature in 20 mM phosphate plus 100 mM NaCl.

Kinetic Studies of the Oxidation of wt and Met16Phe PACu(I) Mutant by the Inorganic Complex $NH_4[Co(dipic)_2]\cdot H_2O$. The complex ammonium bis(pyridine-2,6-dicarboxylato)cobaltate(III) (reduction potential 747 mV vs NHE) was prepared as described previously (*61*) and was characterized from its visible peak at 510 nm ($\epsilon = 630$ M^{-1} cm^{-1}). The oxidation of wt and Met16Phe PACu(I) was monitored at 594 and 598 nm, respectively, on an Applied Photophysics SX.18MV stopped-flow reaction analyzer at 25 °C. All rate constants were obtained under pseudo-first-order conditions (with the inorganic oxidant in greater than 10-fold excess using protein concentrations of 10−30 μM) and were an average of at least five determinations using the same solutions.

The pH dependence of the oxidation of the two proteins by $[Co(dipic)_2]^-$ was studied in the range of pH 6.3−3.8. The studies in the pH range of 6.3−5.4 were carried out in Mes buffer, and sodium acetate buffer was used in the range 5.3 to 3.8 (all at $I = 0.10$ M with NaCl). A pH jump method was used in which the protein was in 1 mM buffer ($I = 0.10$ M, NaCl) in the middle of the pH range covered by the particular buffer, and the $[Co(dipic)_2]^-$ solution was made up in 40 mM buffer ($I = 0.10$ M, NaCl) at the pH that was to be investigated. Check experiments were carried out in which both the complex and the protein were in 20 mM buffer ($I = 0.10$ M, NaCl) at the desired pH value, and identical results were obtained.

RESULTS

UV/Vis Spectra. The UV/vis spectrum of wt PACu(II) at pH 8.0 is shown in Figure 2 and exhibits three intense absorption bands at 453 ($\epsilon = 1600$ M^{-1} cm^{-1}), 594 ($\epsilon = 3700$ M^{-1} cm^{-1}) [both due to the S(Cys)→Cu(II) LMCT transitions], and 758 nm ($\epsilon = 1800$ M^{-1} cm^{-1}). The spectrum of Met16Phe PACu(II) is also shown in Figure 2 (also at pH 8.0) and is different to that of the wt protein. The most intense absorption band is shifted to 598 nm in the mutant,

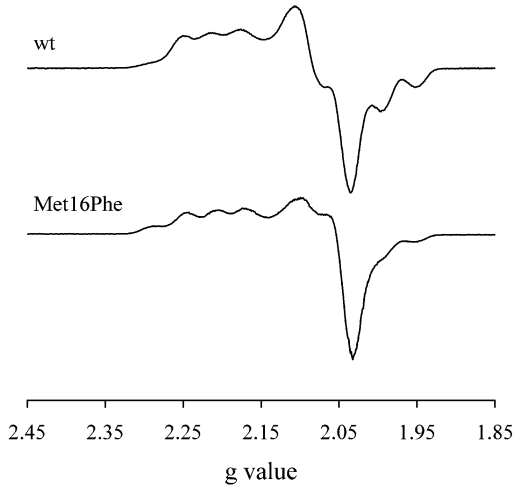

FIGURE 3: X-band EPR spectra of the oxidized proteins in 25 mM Hepes, pH 7.6 (40% glycerol), at −196 °C.

and the molar extinction coefficient increases to 4700 M^{-1} cm^{-1}. The second S(Cys)→Cu(II) LMCT band is also shifted as compared to its position in wt PACu(II) to 459 nm in the Met16Phe variant, and its intensity decreases to 1470 M^{-1} cm^{-1}. This results in a A_{459}/A_{598} ratio of 0.31 for Met16Phe PACu(II) as compared to a A_{453}/A_{594} ratio of 0.43 for wt PACu(II).

The visible spectrum of the Met16Phe mutant is pH-dependent in the range 8.0 to 5.0 as is also the case in wt PACu(II) (*67*). When the pH is lowered from 8.0, the band at 598 nm increases in intensity while that at 459 nm becomes less intense (the position of the bands is unaltered in this pH range). This results in a A_{459}/A_{598} ratio of 0.25 at pH 5.0, and the pH dependence of the A_{459}/A_{598} ratio (data not shown) can be fit (three parameters, nonlinear least squares) to eq 1 corresponding to a two state pH-dependent equilibrium

$$R = (K_a R_H + [H^+]R_L)/(K_a + [H^+]) \quad (1)$$

where R is the observed A_{459}/A_{598} ratio and R_H and R_L are the corresponding ratios at high and low pH, respectively, yielding a pK_a of 6.5 ± 0.1 (R_H and R_L values of 0.31 and 0.25, respectively, were obtained from this fit). The pK_a obtained for this effect in wt PACu(II) is 6.6 ± 0.1 (*67*).

EPR Spectra. The X-band EPR spectra of wt and Met16Phe PACu(II) at pH 7.6 are shown in Figure 3. The spectra of both proteins are almost unaltered by changing pH in the range 10.0 to 3.0 and are rhombic in appearance with that of the Met16Phe variant being slightly more axial. This is confirmed by the EPR parameters [wt PACu(II), $g_x = 2.015$, $A_x = 7.3$ mT, $g_y = 2.053$, $A_y = 1.8$ mT, $g_z = 2.213$, $A_z = 3.5$ mT; Met16Phe PACu(II), $g_x = 2.015$, $A_x = 7.5$ mT, $g_y = 2.043$, $g_z = 2.206$, $A_z = 3.8$ mT] for the two proteins. The simulation of the EPR spectra of both wt and Met16Phe PACu(II) in the g_z region is complicated by the small signal at low field and the apparent lack of a four line hyperfine pattern in this region. Similar features have been observed in the EPR spectra of other cupredoxins, including the PACu from *Alcaligenes faecalis* (*31*, *32*, *38*, *69*−*71*). The g_z and A_z values that are quoted herein are therefore preliminary and are currently the subject of further investigations (errors in these numbers have no impact on the conclusions of the present investigation).

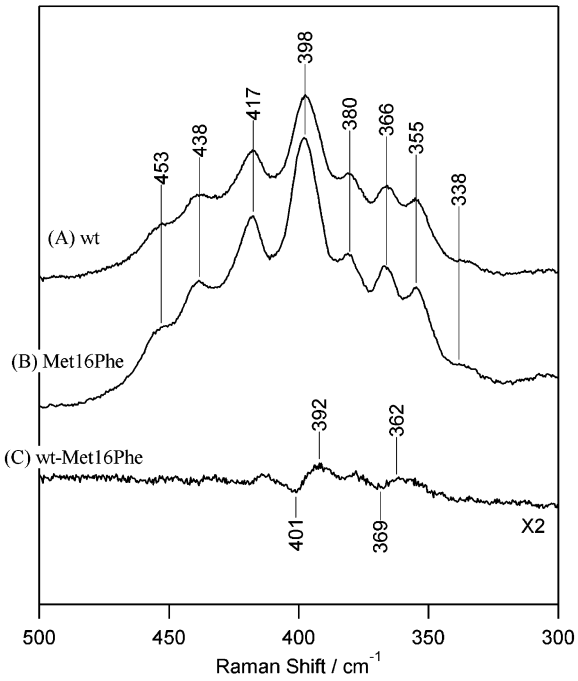

FIGURE 4: RR spectra of (A) wt and (B) Met16Phe PACu(II) in 20 mM phosphate, pH 7.0, under 647 nm excitation at room temperature. Also shown is the difference spectrum obtained by subtracting the Met16Phe spectrum from that of the wt protein (C).

RR Spectra. In Figure 4, the RR spectra of wt PACu(II) and the Met16Phe variant are compared. The large number of bands that occur in this region of the spectrum have been ascribed to kinematic and vibronic coupling of the Cu−S stretch with Cys ligand deformations (*72*). The main band in this region of the RR spectra of type 1 copper sites has been used as an estimate of the Cu−S(Cys) bond strength (*73*). There are slight modifications in the RR spectrum of Met16Phe PACu(II) as compared to the spectrum of the wt protein, and these are highlighted by the difference spectrum shown in Figure 4.

Paramagnetic ^{1}H NMR Spectra. The paramagnetic ^{1}H NMR spectrum of Met16Phe PACu(II) is shown in Figure 5 along with that of the wt protein, and the positions of peaks are listed in Table 1. The directly observed hyperfine shifted resonances in the spectrum of the wt protein have previously been assigned [see Table 1 (*67*)]. In the spectrum of the mutant, most of the shifted resonances are present in almost identical positions as in the wt protein (see Figure 5 and Table 1); thus, we can assume that they arise from the same protons. The main difference between the two spectra is that peak *g*, the Met86 $C^\gamma H$ proton that is found at 13.0 ppm in wt PACu(II), is not observed in the spectrum of the mutant. This signal must exhibit a much smaller hyperfine shift in the spectrum of Met16Phe and is not observed outside of the diamagnetic region.

^{1}H NMR Studies on the Reduced Proteins and the Influence of pH. The ^{1}H NMR spectra of wt and Met16Phe PACu(I) are very similar highlighting that this mutation does not affect the overall structure of PACu. It is interesting to note that the resonance from a methyl group (at 1.73 ppm, data not shown) presumably belonging to Met16 is absent in the spectrum of the Met16Phe mutant and resonances from the

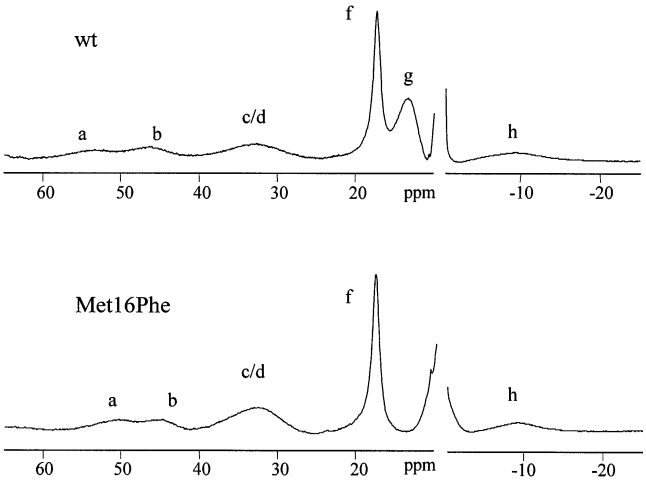

FIGURE 5: ^{1}H NMR spectra (25 °C) of wt PACu(II) and Met16Phe PACu(II) in 10 mM phosphate (99.9% D_2O) at pH* 7.6.

Table 1: Hyperfine Shifted Resonances of wt and Met16Phe PACu(II)[a]

resonance	δ_{obs} (ppm) in wt PACu(II)	δ_{obs} (ppm) in Met16Phe PACu(II)	assignment[b]
a	53.5	51.0	His81 $C^{\delta 2}H$
b	46.0	45.0	His40 $C^{\delta 2}H$
c/d	33.0	32.6	His40/81 $C^{\epsilon 1}H$
e	22.8	23.9	His40 $N^{\epsilon 2}H$
f	17.3	17.8	Asn41 $C^{\alpha}H$
g	13.0	no[c]	Met86 $C^{\gamma}H$
h	−9.7	−9.4	Cys78 $C^{\alpha}H$

[a] Data recorded at 25 °C in 10 mM phosphate buffer at pH 7.6. Also included are the assignments that have been made. [b] For native PACu(II) (*67*). [c] Not observed.

phenyl group of the introduced Phe16 can be identified (at 7.10 and 7.00 ppm, see Figure 6). The region of the spectrum shown in Figure 6 contains the imidazole ring proton resonances ($C^{\delta 2}H$ and $C^{\epsilon 1}H$) from His residues, which appear as singlets (actually unresolved doublets) and can readily be assigned. PACu possesses three His residues at positions 6, 40, and 81, with the latter two being copper ligands. In the spectrum of wt PACu(I) at pH* 6.0 (see Figure 6), the signals at 8.68 and 7.26 ppm have been assigned to the $C^{\epsilon 1}H$ and $C^{\delta 2}H$ resonances of His6, respectively, the peaks at 7.61 and 6.93 to the corresponding protons of His40, and the resonances at 7.28 and 7.08 ppm to those protons of His81 (*67*). Imidazole ring protons from His residues are identified at 8.70, 7.50, 7.35, 7.23, 7.01, and 6.37 ppm at pH* 5.8 in the spectrum of Met16Phe PACu(I) variant (using HSE and CPMG pulse sequences). The signals at 8.70 and 7.23, 7.50 and 7.01, and 7.35 and 6.37 ppm experience cross-peaks in a TOCSY spectrum indicating that these pairs of protons arise from the same His residues. The chemical shifts of the resonances at 8.70 and 7.23 ppm are dependent upon pH* in the range 8.3 to 5.5 (with the position of the peak at 8.70 ppm exhibiting a much larger shift over this pH range) and can be fit to eq 2

$$\delta = (K_a\delta_H + [H^+]\delta_L)/(K_a + [H^+]) \qquad (2)$$

yielding pK_a* values of 7.1 ± 0.1. This pK_a* value is typical of a noncoordinated His residue, and we can thus assign these two signals to His6, with the peak at 8.70 ppm arising from

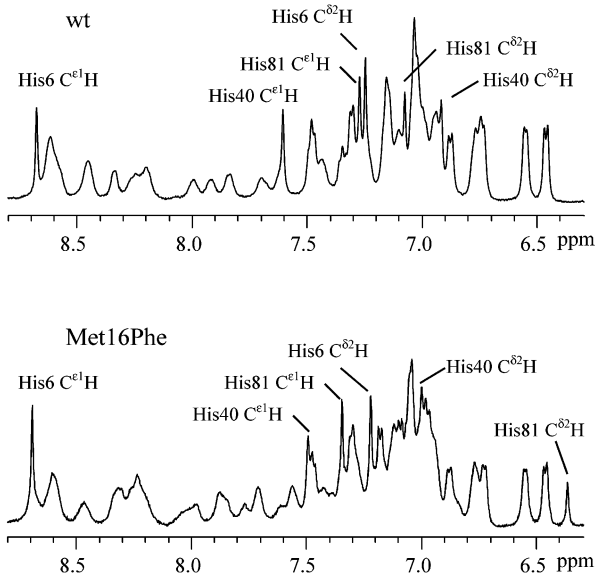

FIGURE 6: Part of the aromatic region of the ^{1}H NMR spectra (25 °C) of wt PACu(I) and Met16Phe PACu(I) in 10 mM phosphate (99.9% D_2O) at pH* 6.0 and 5.8, respectively.

the $C^{\epsilon 1}H$ resonance and that at 7.23 ppm being the $C^{\delta 2}H$ signal. This assignment is supported by the fact that in wt PACu(I) the His6 resonances are found in almost identical positions (vide supra and see Figure 6) and experience a similar pH* dependence also giving rise to a pK_a* of 7.1 ± 0.1 (*67*).

In the NOESY spectrum of Met16Phe PACu(I), the His signals at 7.35 and 7.50 ppm exhibit a strong dipolar connectivity. Such an NOE can only occur between the $C^{\epsilon 1}H$ protons of the two His ligands (His40 and His81), which are situated 2.93 Å apart in the structure of wt PACu(I). Furthermore, a strong NOE is observed between the His $C^{\epsilon 1}H$ signal at 7.50 ppm and the Phe16 resonance at 7.00 ppm, with a weaker NOE observed to the Phe16 peak at 7.10 ppm. The other His $C^{\epsilon 1}H$ signal (at 7.35 ppm) exhibits very weak NOEs to both of the Phe16 resonances (with a slightly stronger NOE observed to the signal at 7.00 ppm). This pattern of NOEs is consistent with the His $C^{\epsilon 1}H$ signal at 7.50 ppm belonging to His40 and that at 7.35 ppm arising from the corresponding signal of His81 [in the crystal structure of the reduced *D. crassirhizoma* plastocyanin one of the $C^{\delta}H$ protons of Phe12 is only 2.1 Å from the His37 $C^{\epsilon 1}H$ proton, whereas distances of ca. >4 Å are observed between protons on the phenyl ring of Phe12 and the imidazole group of His90 (*11*, *12*)]. Thus, the His signal at 7.01 ppm can be assigned to the $C^{\delta 2}H$ of His40 and that at 6.37 ppm to the $C^{\delta 2}H$ of His81. The observed upfield shift of the $C^{\delta 2}H$ of His81, due to ring current effects, is as expected if the phenyl ring of Phe16 is parallel to the imidazole moiety of the histidine and further supports the assignments that we have made. In summary, the positions of most of the His imidazole ring protons are almost unaffected by the Met16Phe mutation. The only exception is the $C^{\delta 2}H$ of His81, which is upfield shifted by ∼0.7 ppm in the mutant as compared to its position in the wt protein.

At pH* values below approximately 6.0, the position of the imidazole ring protons of the His81 ligand in wt PACu(I) start to shift in a downfield direction (see Figure 7). The His81 $C^{\epsilon 1}H$ signal is more affected than the $C^{\delta 2}H$ peak, but

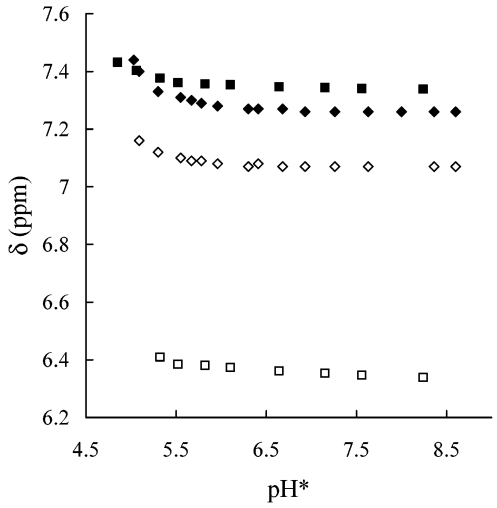

FIGURE 7: Dependence on pH* (25 °C) of the chemical shift of the $C^{\delta 2}H$ (◇) and $C^{\epsilon 1}H$ (◆) resonances of His81 in the ^1H NMR spectrum of wt PACu(I) and the $C^{\delta 2}H$ (□) and $C^{\epsilon 1}H$ (■) resonances of His81 in the ^1H NMR spectrum of Met16Phe PACu(I) in both cases in 10 mM phosphate.

both broaden considerably as the pH* is lowered. This behavior is consistent with protonation of His81, but because neither peak can be observed below pH* 5, fitting of the data to eq 2 is impossible. In the spectrum of the Met16Phe PACu(I) variant, the His81 imidazole ring resonances also start to shift downfield upon lowering the pH* below ~5.5 (see Figure 7). Again, both of the signals broaden dramatically and below pH* 4.8 they cannot be observed (fitting of the data to eq 2 is therefore also impossible).

Reduction Potentials and the Influence of pH. The Met16Phe PACu variant yields good, quasireversible, responses on a 4,4-dithiodipyridine-modified gold electrode in the pH range 8.7 to 5.4. In all cases, the anodic and cathodic peaks are of equal intensity and their separation is approximately 60−80 mV at a scan rate of typically 20 mV/s. The reduction potential at pH 8.2 is 319 mV (vs NHE), and when the pH is lowered to 5.4, a value of 343 mV is obtained. The dependence on pH of the reduction potential of Met16Phe PACu is shown in Figure 8 and can be fit to eq 3:

$$E_m\,(\mathrm{pH}) = E_m\,(\text{low pH}) + (RT/nF)\,\ln[(K_a^{red} + [H^+])/(K_a^{ox} + [H^+])] \quad (3)$$

In eq 3, E_m (pH) is the measured reduction potential, E_m (low pH) is the reduction potential at low pH, K_a^{red} and K_a^{ox} are the proton dissociation constants for the residue in the reduced and oxidized protein, respectively, which influence the E_m (pH) value, and the other symbols have their usual meaning. The fit of the data in Figure 8 to this equation yields pK_a^{red} and pK_a^{ox} values of 7.1 ± 0.1 and 6.6 ± 0.1, respectively.

Kinetics Studies of the Oxidation of wt and Met16Phe PCu(I) by [Co(dipic)$_2$]$^-$. Linear plots of first-order rate constants, k_{obs} (s^{-1}), against [Co(dipic)$_2$]$^-$ concentration (*1*−*15*) × 10^{-4} M for both wt and Met16Phe PACu(I) at pH 6.2 and 4.1 (data not shown) are consistent with the rate law (eq 4).

$$\text{rate} = k_{Co}[\text{PACu(I)}][\text{Co(dipic)}_2^-] \quad (4)$$

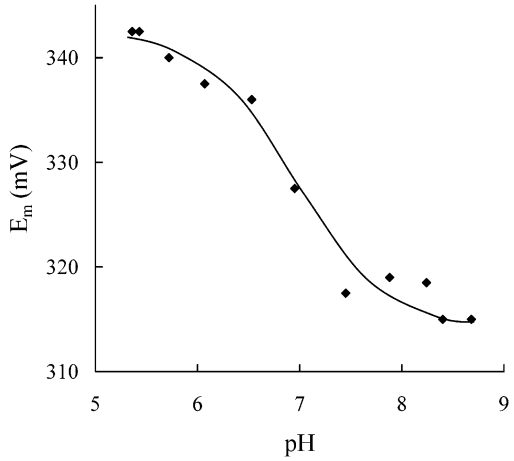

FIGURE 8: Dependence on pH of the reduction potential (E_m) of Met16Phe PACu in 20 mM phosphate plus 100 mM NaCl at room temperature. The line shown is obtained from a fit of the data to eq 3.

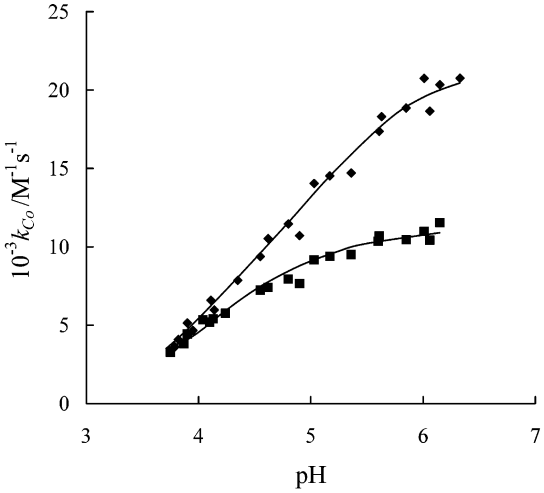

FIGURE 9: Variation of the second-order rate constant (k_{Co}) with pH at 25 °C for the [Co(dipic)$_2$]$^-$ oxidation of wt PACu(I) (◆) and Met16Phe PACu(I) (■) at I = 0.10 M (NaCl). The lines shown are obtained from fits of the data to eq 5.

The variation with pH of the second-order rate constant (k_{Co}) for the oxidation of both proteins is shown in Figure 9, and the dependence of k_{Co} on [H^+] can be analyzed in terms of eq 5

$$k_{Co} = \frac{k_o K_a + k_H[H^+]}{K_a + [H^+]} \quad (5)$$

where the various constants are as defined in eqs 6−8:

$$\text{PACu(I)H}^+ \overset{K_a}{\rightleftharpoons} \text{PACu(I)} + H^+ \quad (6)$$

$$\text{PACu(I)} + \text{Co(III)} \xrightarrow{k_o} \text{PACu(II)} + \text{Co(II)} \quad (7)$$

$$\text{PACu(I)H}^+ + \text{Co(III)} \xrightarrow{k_H} \text{PACu(II)} + \text{Co(II)} + H^+ \quad (8)$$

In the case of wt PACu(I), a pK_a of 4.9 ± 0.1 is obtained and values of 21 010 ± 490 and 3380 ± 510 are found for k_o and k_H, respectively. For Met16Phe PACu(I), the fit of the data in Figure 9 to eq 5 gives 4.5 ± 0.1, 11 020 ± 210, and 2760 ± 430 for pK_a, k_o, and k_H, respectively.

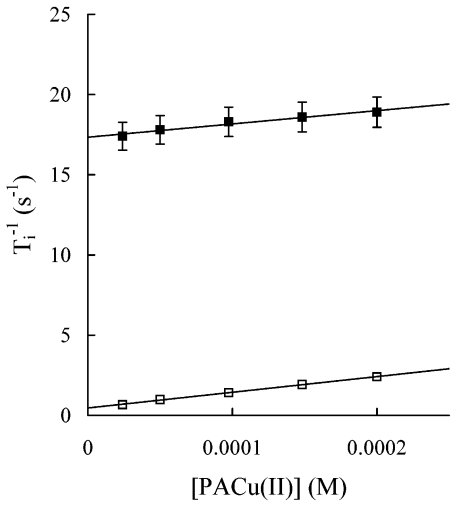

FIGURE 10: Plots of T_1^{-1} (□) and T_2^{-1} (■) against [PACu(II)] for the $C^{\delta 2}H$ signal of His81 (6.35 ppm) in the Met16Phe variant in 37 mM phosphate at pH* 7.6 (25 °C).

ESE Rate Constants. In a mixture of PACu(I) and PACu(II), the slow exchange condition (*74*−*77*) applies to protons that obey the following relationship:

$$k[\mathrm{PACu}]_\mathrm{T} \ll 1/T_{i,\mathrm{ox}} - 1/T_{i,\mathrm{red}} \quad (9)$$

where k is the second-order ESE rate constant, $[\mathrm{PACu}]_\mathrm{T}$ is the total concentration of protein, and $T_{i,\mathrm{ox}}$ and $T_{i,\mathrm{red}}$ ($i = 1$ or 2) are the relaxation times for the oxidized and reduced forms, respectively. In these circumstances for dilute solutions containing only a small proportion (<10%) of the oxidized form of the protein, it can be shown that eq *10* applies (*74*−*77*):

$$1/T_i = (1/T_{i,\mathrm{red}}) + k[\mathrm{PACu(II)}] \quad (10)$$

where T_i is the observed relaxation time of the resonance in the reduced protein and [PACu(II)] is the concentration of PACu(II). Thus, a plot of T_i^{-1} against [PACu(II)] will give a straight line of slope k.

In the studies on the Met16Phe PACu mutant at pH* 7.6, the well-resolved His81 $C^{\delta 2}H$ resonance at 6.35 ppm has been used in the determination of k. The slopes of plots of T_i^{-1} against [PACu(II)] for this resonance (see Figure 10) are 8.3×10^3 M^{-1} s^{-1} for the T_2 data (k_2) and 9.8×10^3 M^{-1} s^{-1} from the T_1 data (k_1). This results in a k_2/k_1 ratio of 0.9 highlighting that this signal is in the slow exchange regime; thus, the k values provide the ESE rate constant [k_2/k_1 ratios of ∼1 are predicted for the slow exchange condition whereas ratios in excess of 5−10 are expected for protons in the fast exchange regime (*74*, *75*)]. The effect of increasing [PACu(II)] on T_2^{-1} is difficult to measure when ESE is so slow, and more precise measurements are achieved from the T_1^{-1} data; thus, the k_1 value provides the most reliable rate constant. Therefore, an ESE rate constant of 9.8×10^3 M^{-1} s^{-1} is obtained at pH* 7.6 for Met16Phe PACu.

It should be noted that all of the above features we have measured for wt PACu (the protein overexpressed in *Escherichia coli*) are identical to those of the native protein (that obtained from *A. cycloclastes*). Therefore, in *E. coli*, the signal sequence of *A. cycloclastes* PACu is successful in transporting the protein to the periplasm and the overexpression host produces correctly folded PACu with the signal peptide removed. The wt protein is contaminated with a very small amount of PACu, which probably possesses Zn(II) at the active site (data not shown).

DISCUSSION

UV/Vis, EPR, RR, and Paramagnetic ^{1}H NMR Spectroscopic Studies. The Met16Phe mutation alters the structure of the copper site of PACu(II), as judged from the spectroscopic studies that we have carried out. The UV/vis and EPR spectra for the mutant are different to those of wt PACu. The change in intensity of the two main LMCT transitions in the visible spectrum of Met16Phe PACu(II) leads to a smaller $A_{\sim 460}/A_{\sim 600}$ ratio as compared to the wt protein. In the EPR spectra, there are slight modifications in the g and A values in the Met16Phe variant, with the most significant alteration being a decrease in the difference between the g_x and g_y values (decreased rhombicity). These features of cupredoxins, decreased rhombicity in the EPR spectrum plus a diminished $A_{\sim 460}/A_{\sim 600}$ ratio in the visible spectrum, can be rationalized with the proposed coupled distortion model (*78*). This model assigns the differences seen in perturbed type 1 copper sites (those with more rhombic EPR spectra and enhanced absorption at around 460 nm in their visible spectra) to an initial shortening of the Cu−S(Met) bond, which results in a tetragonal Jahn−Teller distortion involving coupled rotation of the Cys and Met ligands. We can therefore conclude that the spectroscopic features of the Met16Phe PACu variant indicate an increase in the Cu−S(Met86) bond at the active site and a less tetragonally distorted geometry than that found in the wt protein.

Paramagnetic NMR studies have recently been shown to provide detailed information about the copper site structure of cupredoxins (*66*, *67*, *79*−*85*). In the paramagnetic ^{1}H NMR spectrum of Met16Phe PACu(II), most of the peaks occur in very similar positions as in the wt protein, demonstrating that the active site structure is not drastically altered by this mutation (see Figure 5 and Table 1). The spectrum of Met16Phe PACu(II) does exhibit some subtle differences as compared to that of wt PACu(II). The main dissimilarity between the two spectra is the absence of the $C^\gamma H$ proton resonance of Met86 (peak g) in the spectrum of the Met16Phe protein. This signal must exhibit a considerably smaller hyperfine shift in the mutant. The hyperfine shift is composed of pseudo-contact (dipolar) and Fermi contact (through bond) components, and in cupredoxins, the Fermi contact contribution is much more significant (*79*, *80*). The smaller hyperfine shift of the Met86 $C^\gamma H$ proton in Met16Phe PACu(II) is therefore consistent with a decreased axial Cu(II)−S(Met86) interaction.

The RR spectra of Met16Phe and wt PACu(II) are very similar (see Figure 4). There are some minor alterations in the spectrum of the mutant as compared to the wt protein, and these are highlighted in the difference spectrum shown in Figure 4. The small effect of the Met16Phe mutation on the RR spectrum is consistent with previous studies, which have shown that this technique is relatively insensitive to subtle structural differences at type 1 copper sites (*86*, *87*).

The visible spectrum of Met16Phe PACu(II) is pH-dependent in the range 8.0 to 5.0 (pK_a 6.5 ± 0.1). This behavior is identical to what we have recently observed for

wt PACu(II) (*67*), which is assigned to the protonation of the surface His6 residue. The spectral changes observed upon lowering the pH (a decrease in the A_{459}/A_{598} ratio) indicate that the Cu(II)−S(Met86) interaction is decreased further in the Met16Phe variant under these conditions [His6 protonation also results in a decreased Cu(II)−S(Met86) interaction in the wt protein].

^{1}H NMR Studies on the Reduced Proteins and the Influence of pH. Resonances arising from the imidazole ring protons from all three His residues in Met16Phe PACu(I) have been assigned in the ^{1}H NMR spectrum (see Figure 6). Additionally, two aromatic ring protons from the introduced Phe16 residue have also been identified. The observed NOE pattern between resonances from Phe16 and the two His ligands (His40 and His81) is very similar to what has been observed between His37, His90, and Phe12 resonances in reduced *D. crassirhizoma* plastocyanin (*56*). The upfield shift of the His81 $C^{\delta 2}H$ resonance in Met16Phe PACu(I) results in this proton having an almost identical chemical shift as in reduced *D. crassirhizoma* plastocyanin (*56*). Therefore, the phenyl ring of the introduced Phe16 residue is parallel to the imidazole ring of His81 as is the case for the corresponding groups of Phe12 and His90 in the *D. crassirhizoma* plastocyanin structure (see Figure 1).

The pK_a of 7.1 ± 0.1 for His6 determined in the NMR studies on Met16Phe PACu(I) variant is identical to that of the same residue in the reduced wt protein (*67*). The influence of pH on the chemical shift of the imidazole ring protons of the two His ligands is less revealing in both wt PACu(I) and the reduced Met16Phe variant. The position of the His40 resonances is hardly affected upon lowering the pH* value in both proteins. The His81 $C^{\epsilon 1}H$ and $C^{\delta 2}H$ proton signals shift upon lowering the pH* value (with altering pH* having a greater influence on the $C^{\epsilon 1}H$ peaks) in both wt and Met16Phe PACu(I), but they also broaden, and at pH* values below ca. 5, it is not possible to observe these resonances. This behavior has been observed previously in reduced plastocyanin (*88*) and amicyanin (*59*, *89*) and is consistent with protonation of the His81 ligand, with the broadening due to either an intermediate rate of exchange between the protonated and the deprotonated forms of the His or the presence of two forms of the protonated His that are exchanging at an intermediate rate on the NMR time scale. In amicyanin and plastocyanin, the broadening at acidic pH* values is not as severe as in PACu(I) allowing a more complete titration curve to be obtained. However, the excessive broadening of the His81 imidazole ring resonances in both wt and Met16Phe PACu(I) prevents the use of NMR spectroscopy for determining the pK_a value of this residue. Nevertheless, the data shown in Figure 7 for the His81 $C^{\epsilon 1}H$ proton signals in the two proteins indicate that the pK_a of His81 is lower in the Met16Phe variant. Thus, it would appear that the introduction of a $\pi-\pi$ interaction between the imidazole ring of His81 and the phenyl ring of Phe16 stabilizes the Cu(I)−N(His81) interaction in PACu (vide infra).

Reduction Potentials and the Influence of pH. The reduction potential of Met16Phe PACu is 319 mV at pH 8.2, which compares to a value of 263 mV at pH 8.1 for the wt protein (*67*). The 56 mV increase in the reduction potential indicates that the introduction of a Phe at position 16 stabilizes the Cu(I) form of the protein over the oxidized state. This effect could be due to increased hydrophobicity at the copper center in the Met16Phe variant or it may be that the subtle structural changes at the active site result in the mutant being able to better accommodate the cuprous ion. The 24 mV increase in the reduction potential of the Met16Phe variant upon going to pH 5.4 can be assigned to the influence of the protonation of His6, as is the case for the wt PACu (*67*). From the fit of the data in Figure 8, the pK_a^{red} value (7.1 ± 0.1) is the same as that obtained for His6 from the NMR experiments and is similar to that determined in the electrochemical studies on wt PACu (*67*). The pK_a^{ox} value (6.6 ± 0.1) is very similar to that obtained from the influence of pH on the visible spectrum of Met16Phe PACu(II) and also to that determined from the pH dependence of the reduction potential of the wt protein (*67*). The effect of the oxidation state of the copper ion on the pK_a of His6 is completely consistent with its distance from the active site. The reduction potential of PACu should also be strongly influenced by the protonation of the His81 ligand (*56*, *58*, *63*, *64*). However, the electrochemical response of PACu at a modified gold electrode deteriorates dramatically below pH 5.5 and so this technique is unable to provide information about the influence of the Met16Phe mutation on the pK_a of His81 in PACu(I).

Kinetics Studies of the Oxidation of wt and Met16Phe PACu(I) by [Co(dipic)$_2$]$^-$. The second-order rate constant for the oxidation of Met16Phe PACu(I) by $[Co(dipic)_2]^-$ is considerably smaller than that for the wt protein at pH 6 (see Figure 9). This diminished reactivity is due to the decreased driving force for the ET reaction in the Met16Phe variant as a consequence of the increase in the reduction potential in the mutant {the reduction potential of the $[Co(dipic)_2]^{-/2-}$ couple is 747 mV (*61*)}. The analysis of the influence of pH on the kinetics of the oxidation of PACu(I) is the only approach that has successfully been used to determine the pK_a value of His81 (*60*, *61*). The protonation of the His ligand in the reduced protein leads to a drastic decrease in the second-order rate constant for the oxidation, as the pH value is lowered. This method has also been used to determine the pK_a value of the protonating His ligand in reduced amicyanin (*90*) and plastocyanin (*91*) with the results completely consistent with those from NMR and electrochemical studies. The fits of the data shown in Figure 9 result in pK_a values of 4.9 and 4.5 for His81 in wt and Met16Phe PACu(I), respectively.

Summary of pH-Dependent Measurements. The protonation of the surface His6 residue ($pK_a^{ox} \approx 6.6$, $pK_a^{red} \approx 7.1$), which is situated some 15 Å from the copper ion, affects the visible spectrum and the reduction potential of Met16Phe PACu in a manner similar to that observed previously for the wt protein (*67*). A second and more relevant pH effect in the context of the present study concerns the protonation of the His81 ligand in the reduced protein. The results of the ^{1}H NMR experiments indicate that the pK_a of His81 is lower in the Met16Phe variant than the wt protein, but because of the broadening of resonances at low pH, it is not possible to quantify the difference with this approach. The effect of pH on the kinetics of the oxidation of wt and Met16Phe PACu(I) provides pK_a values of 4.9 and 4.5, respectively, for His81.

Rationalization of the Influence of the Met16Phe Mutation on the pK_a of His81. As stated above, the Met16Phe mutation leads to a decrease of 0.4 pH units in the pK_a of His81 in

PACu(I). Thus, the introduced aromatic ring of Phe16, which is involved in a $\pi-\pi$ contact with the imidazole ring of His81, results in a significant increase in the stability of the Cu(I)−N(His81) interaction. In the case of *D. crassirhizoma* plastocyanin, the contact of the imidazole ring of the His90 residue with the phenyl group of Phe12 also results in stabilization of the Cu(I)−N(His90) interaction and protonation of His90 is not observed in the accessible pH range (*56*). It is interesting to note that in the Leu12Phe variant of spinach plastocyanin [a Leu is found at position 12 in all other plastocyanins except the *D. crassirhizoma* protein and the *Prochlorothrix hollandica* protein where it is a Pro (*92*)], the pK_a of the C-terminal His ligand increases to 5.7 (as compared to 4.8 in the wt protein). NMR studies on this mutant show that the introduced phenyl ring is positioned parallel to the imidazole ring of the His ligand (the His87 $C^{\delta 2}H$ proton resonance experiences a large upfield shift). However, the clear pattern of NOEs between the introduced Phe and the imidazole ring protons of the two His ligands observed in the NOESY spectra of Met16Phe PACu(I) and reduced *D. crassirhizoma* plastocyanin is not present in the spectrum of the Leu12Phe spinach plastocyanin mutant. This indicates that in the Leu12Phe variant a different structural arrangement prevails in this region of the protein, which actually destabilizes the Cu(I)−N(His87) interaction. Initial modeling studies indicate that the imidazole and phenyl rings will be offset in the Met16Phe PACu variant, as in the structure of the *D. crassirhizoma* plastocyanin (*11*, *12*), whereas in the Leu12Phe plastocyanin variant the two ring systems may overlap more completely. These observations are consistent with the nature of $\pi-\pi$ interactions as postulated by Hunter and Sanders (*50*), whereby a more favorable attractive force is obtained when parallel π-systems are offset rather than having a direct face-to-face geometry.

ESE Reactivity. The ESE rate constant of Met16Phe PACu is 9.8×10^3 M^{-1} s^{-1} at pH* 7.6, which compares with a value of 3.7×10^3 M^{-1} s^{-1} for the wt protein (*67*) under identical conditions. The approximately 2.5-fold increase in the ESE rate constant as a consequence of the introduction of a Phe residue adjacent to the side chain of His81 is an intriguing result of this study. The mutation has produced a PACu, which is more efficient than the wt protein at the task that it was designed for, biological ET. The reason for the enhanced ET reactivity of the mutant protein can be attributed to the $\pi-\pi$ interaction of the introduced phenyl ring and the coordinated His81 imidazole, enhancing the rigidity of the copper site environment and thus lowering its reorganization energy (the effect of the Met16Phe mutation on the ESE rate constant equates to an approximately 90 meV decrease in the reorganization energy). It could also be that the increased ESE reactivity in the Met16Phe variant is due to a decreased distance for ET in the encounter complex or that protein−protein association is facilitated (the observed effect would equate to a ca. 0.7 Å decrease in the distance for ET or an ∼2 kJ/mol relative increase in the Gibbs free energy of association of two PACu molecules).

CONCLUSIONS

The Met16Phe mutation has a modest effect on the spectroscopic properties, and thus the structure, of the active site of PACu(II). The results of all of the spectroscopic studies are consistent with a lengthening of the Cu(II)−S(Met86) bond in the Met16Phe variant. These results demonstrate that residues in the second coordination environment of a type 1 copper site exert a degree of control over the structure of the active site. The aromatic ring of the introduced Phe16 residue is involved in a $\pi-\pi$ interaction with the imidazole ring of His81 and therefore mimics the contact observed in the structure of *D. crassirhizoma* plastocyanin. This stabilizes the Cu(I)−N(His81) interaction and produces a copper site that is more efficient at ET.

ACKNOWLEDGMENT

We thank Dr. Tony Royston (University of Durham, U.K.) for assistance with EPR spectroscopy and are grateful to Prof. T. Kitagawa for access to RR facilities through the Joint Studies Program (2001−2002) of the Institute for Molecular Science, Okazaki, Japan.

SUPPORTING INFORMATION AVAILABLE

Experimental procedures describing cell growth and protein expression, isolation and purification of proteins, and NMR spectroscopy. This material is available free of charge via the Internet at http://pubs.acs.org.

REFERENCES

1. Kakutami, T., Watanabe, H., Arima, K., and Beppu, T. (1981) *J. Biochem. 89*, 463−472.
2. Liu, M. Y., Liu, M. C., Payne, W. J., and Legall, J. (1986) *J. Bacteriol. 166*, 604−608.
3. Moir, J. W. B., Baratta, D., Richardson, D. J., and Ferguson, S. J. (1993) *Eur. J. Biochem. 212*, 377−385.
4. Petratos, K., Dauter, Z., and Wilson, K. S. (1988) *Acta Crystallogr. B44*, 628−636.
5. Adman, E. T., Turley, S., Bramson, R., Petratos, K., Banner, D., Tsernoglou, D., Beppu, T., and Watanabe, H. (1989) *J. Biol. Chem. 264*, 87−99.
6. Vakoufari, E., Wilson, K. S., and Petratos, K. (1994) *FEBS Lett. 347*, 203−206.
7. Inoue, T., Kai, Y., Harada, S., Kasai, N., Ohshiro, Y., Suzuki, S., Kohzuma, T., and Tobari, J. (1994) *Acta Crystallogr. D50*, 317−328.
8. Inoue, T., Nishio, N., Suzuki, S., Kataoka, K., Kohzuma, T., and Kai, Y. (1999) *J. Biol. Chem. 274*, 17845−17852.
9. Williams, P. A., Fülöp, V., Leung, Y. C., Chan, C., Moir, J. W. B., Howlett, G., Ferguson, S. J., Radford, S. E., and Hajdu, J. (1999) *Nat. Struct. Biol. 2*, 975−982.
10. Thompson, G. S., Leung, Y. C., Ferguson, S. J., Radford, S. E., and Redfield, C. (2000) *Protein Sci. 9*, 846−858.
11. Kohzuma, T., Inoue, T., Yoshizaki, F., Sasakawa, Y., Onodera, K., Nagatomo, S., Kitagawa, T., Uzawa, S., Isobe, Y., Sugimura, Y., Gotowda, M., and Kai, Y. (1999) *J. Biol. Chem. 274*, 11817−11823.
12. Inoue, T., Gotowda, M., Sugawara, H., Kohzuma, T., Yoshizaki, F., Sugimura, Y., and Kai, Y. (1999) *Biochemistry 38*, 13853−13861.
13. Kraulis, P. J. (1991) *J. Appl. Crystallogr. 24*, 946−950.
14. Kukimoto, M., Nishiyama, M., Tanokura, M., Adman, E. T., and Horinouchi, S. (1996) *J. Biol. Chem. 271*, 13680−13683.
15. Kukimoto, M., Nishiyama, M., Ohnuki, T., Turley, S., Adman, E. T., Horinouchi, S., and Beppu, T. (1995) *Protein Eng. 8*, 153−158.
16. Chen, L., Durley, R., Poliks, B. J., Hamada, K., Chen, Z., Mathews, F. S., Davidson, V. L., Satow, Y., Huizinga, E., Vellieux, F. M. D., and Hol, W. G. J. (1992) *Biochemistry 31*, 4959−4964.
17. Ubbink, M., Ejdeback, M., Karlsson, B. G., and Bendall, D. S. (1998) *Structure 6*, 323−335.
18. van de Kamp, M., Floris, R., Hali, F. C., and Canters, G. W. (1990) *J. Am. Chem. Soc. 112*, 907−908.
19. Kyritsis, P., Dennison, C., Ingledew, W. J., McFarlane, W., and Sykes, A. G. (1995) *Inorg. Chem. 34*, 5370−5374.

20. Dennison, C., and Kohzuma, T. (1999) *Inorg. Chem. 38*, 1491−1497.
21. Canters, G. W., and Gilardi, G. (1993) *FEBS Lett. 325*, 39−48.
22. Solomon, E. I., Penfield, K. W., Gewirth, A. A., Lowery, M. D., Shadle, S. E., Guckert, J. A., and LaCroix, L. B. (1996) *Inorg. Chim. Acta 243*, 67−78.
23. Mizoguchi, T. J., DiBilio, A. J., Gray, H. B., and Richards, J. H. (1992) *J. Am. Chem. Soc. 114*, 10076−10078.
24. Karlsson, B. G., Nordling, M., Pascher, T., Tsai, L. C., Sjölin, L., and Lundberg, L. G. (1991) *Protein Eng. 4*, 343−349.
25. Romero, A., Hoitink, C. W. G., Nar, H., Huber, R., Messerschmidt, A., and Canters, G. W. (1993) *J. Mol. Biol. 229*, 1007−1021.
26. Germanas, J. P., DiBilio, A. J., Gray, H. B., and Richards, J. H. (1993) *Biochemistry 32*, 7698−7702.
27. Karlsson, B. G., Tsai, L. C., Nar, H., Sanders-Loehr, J., Bonander, N., Langer, V., and Sjölin, L. (1997) *Biochemistry 36*, 4089−4095.
28. Messerschmidt, A., Prade, L., Kroes, S. J., Sanders-Loehr, J., Huber, R., and Canters, G. W. (1998) *Proc. Natl. Acad. Sci. U.S.A. 95*, 3443−3448.
29. van Pouderoyen, G., Andrew, C. R., Loehr, T. M., Sanders-Loehr, J., Mazumdar, S., Hill, H. A. O., and Canters, G. W. (1996) *Biochemistry 35*, 1397−1407.
30. den Blaauwen, T., and Canters, G. W. (1993) *J. Am. Chem. Soc. 115*, 1121−1129.
31. Casimiro, D. R., Toy-Palmer, A., Blake, R. C., and Dyson, H. J. (1995) *Biochemistry 34*, 6640−6648.
32. Hall, J. F., Kanbi, L. D., Strange, R. W., and Hasnain, S. S. (1999) *Biochemistry 38*, 12675−12680.
33. Diederix, R. E. M., Canters, G. W., and Dennison, C. (2000) *Biochemistry 39*, 9551−9560.
34. Williams, R. J. P. (1995) *Eur. J. Biochem. 234*, 363−381.
35. Malmström, B. G. (1994) *Eur. J. Biochem. 223*, 711−718.
36. Hoitink, C. W. G., and Canters, G. W. (1992) *J. Biol. Chem. 267*, 13836−13842.
37. Dong, S., Ybe, J. A., Hecht, M. H., and Spiro, T. G. (1999) *Biochemistry 38*, 3379−3385.
38. Hall, J. F., Kanbi, L. D., Harvey, I., Murphy, L. M., and Hasnain, S. S. (1998) *Biochemistry 37*, 11451−11458.
39. Nishiyama, M., Suzuki, J., Ohnuki, T., Chang, H. C., Horinouchi, S., Turley, S., Adman, E. T., and Beppu, T. (1992) *Protein Eng. 5*, 177−184.
40. Libeu, C. A. P., Kukimoto, M., Nishiyama, M., Horinouchi, S., and Adman, E. T. (1997) *Biochemistry 36*, 13160−13179.
41. Machczynski, M. C., Gray, H. B., and Richards, J. H. (2002) *J. Inorg. Biochem. 88*, 375−380.
42. Adman, E. T. (1991) *Adv. Protein Chem. 42*, 145−197.
43. Tsai, L. C., Sjölin, L., Langer, V., Pascher, T. and Nar, H. (1995) *Acta Crystallogr. D51*, 168−176.
44. Hart, P. J., Nersissian, A. M., Herrmann, R. G., Nalbandyan, R. M., Valentine, J. S., and Eisenberg, D. (1996) *Protein Sci. 5*, 2175−2183.
45. Zarić, S. D., Popović, D. M., and Knapp, E. W. (2000) *Chem. Eur. J. 6*, 3935−3942.
46. Dougherty, D. A. (1996) *Science 271*, 163−168.
47. Dickerson, R. E. (1992) *Methods Enzymol. 211*, 67−111.
48. Tsai, C. C., Jain, S. C., and Sobell, H. M. (1975) *Proc. Natl. Acad. Sci. U.S.A. 72*, 628−632.
49. Creighton, T. E. (1993) *Proteins − Structures and Molecular Properties*, 2nd ed., W. H. Freeman and Company, New York.
50. Hunter, C. A., and Sanders, J. K. M. (1990) *J. Am. Chem. Soc. 112*, 5525−5534.
51. Yamauchi, O., Odani, A., Kohzuma, T., Masuda, H., Toriumi, K., and Saito, K. (1989) *Inorg. Chem. 28*, 4066−4068.
52. Yamauchi, O., Odani, A., and Takani, M. (2002) *J. Chem. Soc., Dalton Trans.* 3411−3421.
53. Yamauchi, O., Odani, A., and Hirota, S. (2001) *Bull. Chem. Soc. Jpn. 74*, 1525−1545.
54. Yajima, T., Okajima, M., Odani, A., and Yamauchi, O. (2002) *Inorg. Chim. Acta 339*, 445−454.
55. Meyer, E. A., Castellano, R. K., and Diederich, F. (2003) *Angew. Chem., Int. Ed. 42*, 1210−1250.
56. Dennison, C., Lawler, A. T., and Kohzuma, T. (2002) *Biochemistry 41*, 552−560.
57. Guss, J. M., Harrowell, P. R., Murata, M., Norris, V. A., and Freeman, H. C. (1986) *J. Mol. Biol. 192*, 361−387.
58. Battistuzzi, G., Borsari, M., Canters, G. W., de Waal, E., Leonardi, A., Ranieri, A., and Sola, M. (2002) *Biochemistry 41*, 14293−14298.
59. Lommen, A., and Canters, G. W. (1990) *J. Biol. Chem. 265*, 2768−2774.
60. Dennison, C., Kohzuma, T., McFarlane, W., Suzuki, S., and Sykes, A. G. (1994) *Chem. Commun*. 581−582.
61. Dennison, C., Kohzuma, T., McFarlane, W., Suzuki, S., and Sykes, A. G. (1994) *Inorg. Chem. 33*, 3299−3305.
62. Zhu, Z., Cunane, L. M., Chen, Z. W., Durley, R. C. E., Mathews, F. S., and Davidson, V. L. (1998) *Biochemistry 37*, 17128−17136.
63. Armstrong, F. A., Hill, H. A. O., Oliver, B. N., and Whitford, D. (1985) *J. Am. Chem. Soc. 107*, 1473−1476.
64. Dennison, C., Vijgenboom, E., Hagen, W. R., and Canters, G. W. (1996) *J. Am. Chem. Soc. 118*, 7406−7407.
65. DiBilio, A. J., Dennison, C., Gray, H. B., Ramirez, B. E., Sykes, A. G., and Winkler, J. R. (1998) *J. Am. Chem. Soc. 120*, 7551−7556.
66. Sato, K., Kohzuma, T., and Dennison, C. (2003) *J. Am. Chem. Soc. 125*, 2101−2112.
67. Sato, K., and Dennison, C. (2002) *Biochemistry 41*, 120−130.
68. Chen, Y. C., Chang, W. C., Chang, T., Chang, W. C., Liu, M. Y., Payne, W. J., and LeGall, J. (1996) *Biochem. Biophys. Res. Commun. 219*, 423−428.
69. Cox, J. C., Aasa, R., and Malmström, B. G. (1978) *FEBS Lett. 93*, 157−160.
70. Kakutami, T., Watanabe, H., Arima, K., and Beppu, T. (1981) *J. Biochem. 89*, 463−472.
71. Nunzi, F., Guerlesquin, F., Shepard, W., Guigliarelli, B., and Bruschi, M. (1994) *Biochem. Biophys. Res. Commun. 203*, 1655−1662.
72. Han, J., Adman, E. T., Beppu, T., Codd, R., Freeman, H. C., Huq, L., Loehr, T. M., and Sanders-Loehr, J. (1991) *Biochemistry 30*, 10904−10913.
73. Andrew, C. R., Yeom, H., Valentine, J. S., Karlsson, B. G., Bonander, N., van Pouderoyen, G., Canters, G. W., Loehr, T. M., and Sanders-Loehr, J. (1994) *J. Am. Chem. Soc. 116*, 11489−11498.
74. Groeneveld, C. M., and Canters, G. W. (1988) *J. Biol. Chem. 263*, 167−173.
75. Dennison, C., Kyritsis, P., McFarlane, W., and Sykes, A. G. (1993) *J. Chem. Soc., Dalton Trans.* 1959−1963.
76. Leigh, J. S. (1971) *J. Magn. Reson. 4*, 308−311.
77. McLaughlin, A. C., and Leigh, J. S. (1973) *J. Magn. Reson. 9*, 296−304.
78. LaCroix, L. B., Shadle, S. E., Wang, Y., Averill, B. A., Hedman, B., Hodgson, K. O., and Solomon, E. I. (1996) *J. Am. Chem. Soc. 118*, 7755−7768.
79. Kalverda, A. P., Salgado, J., Dennison, C., and Canters, G. W. (1996) *Biochemistry 35*, 3085−3092.
80. Bertini, I., Ciurli, S., Dikiy, A., Gasanov, R., Luchinat, C., Martini, G., and Safarov, N. (1999) *J. Am. Chem. Soc. 121*, 2037−2046.
81. Bertini, I., Fernández, C. O., Karlsson, B. G., Leckner, J., Luchinat, C., Malmström, B. G., Nersissian, A. M., Pierattelli, R., Shipp, E., Valentine, J. S., and Vila, A. J. (2000) *J. Am. Chem. Soc. 122*, 3701−3707.
82. Dennison, C., Oda, K., and Kohzuma, T. (2000) *Chem. Commun*. 751−752.
83. Bertini, I., Ciurli, S., Dikiy, A., Fernandez, C. O., Luchinat, C., Safarov, N., Shumilin, S., and Vila, A. J. (2001) *J. Am. Chem. Soc. 123*, 2405−2413.
84. Dennison, C., and Lawler, A. T. (2001) *Biochemistry 40*, 3158−3166.
85. Dennison, C., Harrison, M. D., and Lawler, A. T. (2003) *Biochem. J. 371*, 377−383.
86. den Blaauwen, T., Hoitink, C. W. G., Canters, G. W., Han, J., Loehr, T. M., and Sanders-Loehr, J. (1993) *Biochemistry 32*, 12455−12464.
87. Buning, C., Canters, G. W., Comba, P., Dennison, C., Jeuken, L., Melter, M., and Sanders-Loehr, J. (2000) *J. Am. Chem. Soc. 122*, 204−211.
88. Kojiro, C. L., and Markley, J. L. (1983) *FEBS Lett. 162*, 52−56.
89. Jeuken, L. J. C., Camba, R., Armstrong, F. A., and Canters, G. W. (2002) *J. Biol. Inorg. Chem. 7*, 94−100.
90. Kyritsis, P., Dennison, C., Kalverda, A. P., Canters, G. W., and Sykes, A. G. (1994) *J. Chem. Soc., Dalton Trans.* 3017−3023.
91. Segal, M. G., and Sykes, A. G. (1978) *J. Am. Chem. Soc. 100*, 4585−4592.
92. Babu, C. R., Volkman, B. F., and Bullerjahn, G. S. (1999) *Biochemistry 38*, 4988−4995.

BI030030P